Modelling of an Optical Access Network Platform for Radio-Frequency Transmission in the S Band

Modelação de uma Plataforma de Rede de Acesso Óptico para Transmissão de Radiofrequências na Banda S

DOI:10.34117/bjdv7n8-227

Recebimento dos originais: 10/07/2021
Aceitação para publicação: 10/08/2021

Flávio André Nogueira Sampaio
Engenheiro de Telecomunicações (UFF)
Orange Labs
Endereço: 2 Avenue Pierre Marzin, CEP 22300, Lannion, France

Pedro Santos Abreu
Engenheiro de Telecomunicações (UFF)
Escola de Engenharia, Universidade Federal Fluminense
Endereço: Rua Passo da Pátria, 156, bloco E sala 406, CEP 24210-240, Niterói, RJ

Vinicius Nunes Henrique Silva
Ph.D. em Engenharia de Telecomunicações (Telecom Bretagne)
Universidade de Coimbra
Instituto de Telecomunicações, CEP 3030-290, Coimbra, Portugal

Tadeu Nagashima Ferreira
D.Sc. em Engenharia Elétrica (UFRJ)
Escola de Engenharia, Universidade Federal Fluminense
Endereço: Rua Passo da Pátria, 156, bloco E sala 406, CEP 24210-240, Niterói, RJ
E-mail: tadeu_ferreira@id.uff.br

Luiz Anet Neto
PhD in Hyperfrequency Electronics and Optoelectronics (Université de Limoges)
Optics Department, IMT Atlantique
Campus de Brest, Technopôle Brest-Iroise, CEP 29238, Brest, France

Alberto Gaspar Guimarães
D.Sc. em Engenharia Elétrica (PUC-Rio)
Escola de Engenharia, Universidade Federal Fluminense
Endereço: Rua Passo da Pátria, 156, bloco E sala 406, CEP 24210-240, Niterói, RJ

Vanessa Przybylski Ribeiro Magri
D.Sc. em Engenharia Elétrica (PUC-Rio)
Escola de Engenharia, Universidade Federal Fluminense
Endereço: Rua Passo da Pátria, 156, bloco E sala 406, CEP 24210-240, Niterói, RJ

Andrés Pablo López Barbero
D.Sc. em Engenharia Elétrica (UNICAMP)
Escola de Engenharia, Universidade Federal Fluminense

Endereço: Rua Passo da Pátria, 156, bloco E sala 406, CEP 24210-240, Niterói, RJ

ABSTRACT
Microwave transmission in the S Band are used in WiMAX, mobile telephony, air control and satellite communications. Such applications demand the use of wideband optical access networks. In this article, the impact of non-linearities of a fluorescent optical source (FFOS) is analyzed on the performance, at 560 nm, of Discrete-Multitone (DMT) transmissions, using the multicarrier signal-to-noise ratio (SNR_{mc}) metric. The objective is to provide a model of SNR_{mc} level curves based on empirical measurements by varying the bias current and the amplitude of the input signal in the optical source. The cartography was approximated by fitting ellipses, which allows us to find an approximate optimum point of operation for the setup.

Keywords: Fluorescent Optical Source, Discrete Multitone, POF.

RESUMO
A transmissão de micro-ondas na Banda S é utilizada em WiMAX, telefonia móvel, controlo aéreo e comunicações via satélite. Tais aplicações exigem a utilização de redes de acesso óptico de banda larga. Neste artigo, o impacto das não linearidades de uma fonte óptica fluorescente (FFOS) é analisado no desempenho, a 560 nm, das transmissões de DMT (Discrete-Multitone), utilizando a métrica de relação sinal/ruído (SNRmc) de multicarrier. O objectivo é fornecer um modelo de curvas de nível SNRmc baseado em medições empíricas, variando a corrente de polarização e a amplitude do sinal de entrada na fonte óptica. A cartografia foi aproximada através da montagem de elipses, o que nos permite encontrar um ponto de funcionamento óptimo aproximado para a configuração.

Palavras-chave: Fonte Óptica Fluorescente, Multitone Discreto, POF.

1 INTRODUCTION

The use of the S-band for microwave communications includes several applications, such as, IEEE 802.16m (Wi-MAX), fifth generation (5G) mobile telephony, air traffic control and satellite communications. All these applications require very high rates in the transmission. Then, the transmission on the access network should be performed in optical fibers.

New generations of communication systems demand an exponentially increasing growth of data rates. Optical fiber communications are a common solution to the datalink bottleneck, especially on the last mile. Optical sources have been proposed based on fast wavelength conversion [1], where a 560-nm light source composed by a fluorescent plastic optical fiber (FPOF) is pumped by a co-propagating source at 520 nm, generated by a green light-emitting diode (LED). Afterwards, the use of a wavelength-converted optical carrier at 560 nm was experimentally assessed for 120 Mb/s with discrete multitone (DMT) data communication [2], [3], [4]. Spectral efficiency of 6 bits/s/Hz has

been achieved over 20 m of step index plastic optical fiber (SI-POF) for a pre-forward error correction (FEC) target bit-error rate (BER) of 10^{-3}.

The use of step-index polymethylmethacrylate (SI-PMMA) fibers provides plenty of advantages, such as ease of handling, low cost and robustness to electromagnetic interference (EMI). On the other hand, the plastic optical fiber (POF) presents high modal dispersion profile and attenuation, which limits the communication link bandwidth and its length to the order of 50 MHz for 100 m [5], [6], [7]. These characteristics support using POF in the scenario of short-ranged applications such as multimedia communications, intra-vehicular devices and domestic networks [8], [9], [10], [11].

Wavelength-division multiplex (WDM) is a consolidated technology for silica fibers which shows huge potential to increase the transmission rate for domestic network links, however it has not been implemented commercially yet in POFs since its insertion loss is high [12], [13].

It is possible to increase the capacity of a WDM system by adding a new optical source or improving the single transmission channel. Since the attenuation profile of a PMMA POF depends on its inherent characteristics, then increasing the transmission rates per wavelength implies changing the multiplexing or modulation technique [14]. The Discrete Multitone (DMT) is a well-known spectrally efficient multicarrier transmission technique and it has been implemented recently for some optical systems in order to achieve higher bit data rates [14]. Concerning multiplexing, several implementations of WDM techniques have been proposed recently [15], [16], [17], [18]. However, none of them exploits the yellow/orange transmission window since semiconductors such as GaAsP and GaP:N are not commonly integrated with fiber [12].

In some previous works [3], [4], data rates have been achieved up to 128 Mb/s for a pre-FEC target BER of 10^{-3} over 20 m of SI-POF for FPOF with intensity modulation and direct detection (IM/DD). Moreover, that implementation reached spectral efficiency as high as 6.39 bits/s/Hz and aggregated rough data bit rates up to 455 Mb/s using four optical sources operating on the main transmission windows of the POF [3]. In [4], channel non-linearities are addressed by varying the bias current and the amplitude of the electrical modulating signal by a scaling factor (SF) in terms of the multicarrier signal-to-noise ratio (SNR_{mc}) in an optical back-to-back configuration (OB2B).

In this article, the performance of an optical channel is assessed in 20 m of SI-POF PMMA. The main objective of this article is to model the SNR_{mc} as a metric in our DMT transmission setup using bias current and SF as input variables and find a closely

optimal operating point. The SNR_{mc} is plotted as level curves in two-dimensional diagrams of SF and bias current, where an eliptical fitting of the cartography is performed.

Section 2 presents the DMT transmission system considered here for optical communications. In Section 3, some specific characteristics of the DMT system are presented. Section 4 shows the experimental setup used in the measurement campaign. In Section 5, the results are presented. Section 6 concludes the article.

2 DMT TRANSMISSION CHANNEL

Figure 1 shows the DMT transmission scheme used in this article. A higher-rate serial pseudorandom binary sequence (PRBS) stream is generated. Then, it is parallelized into lower bit-rate sequences which are mapped into M-ary quadrature amplitude modulation (M-QAM) symbols, which modulate DMT subcarriers, by using the IFFT (inverse Fast Fourier Transform). The transmitted signal is desired to be strictly real so the input block to the IFFT presents a Hermitian symmetry at each instant [19]. Afterwards, a cyclic prefix (CP) is added to allow extra robustness to intersymbol interference (ISI). The signal is serialized before generating an analog signal by a digital-to-analog converter (DAC).

For Laser Diodes, it is relatively simple to find a typical region above the current threshold and below the maximum saturation bias for one static assessment of the source, without the signal being modulated. With this estimation, a more precise assessment can be done by measuring third-order intermodulation (IM3) distortion using two sinusoidal signals [15].

Figure 1: DMT modulation and demodulation scheme.

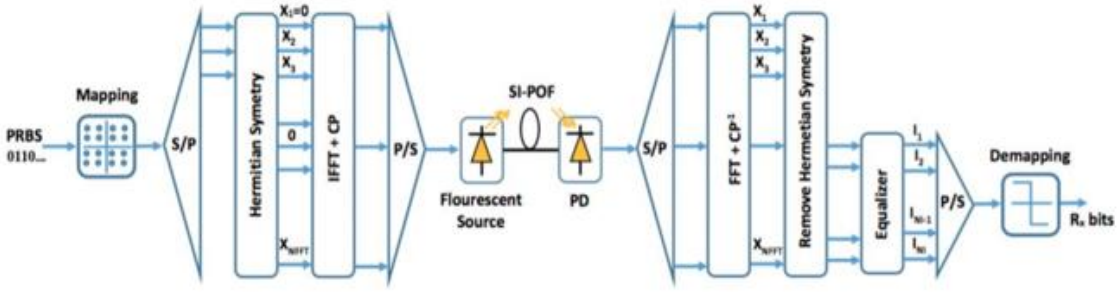

Some light sources, such as Light Emitting Diodes (LEDs), do not have distinguishable linear regions [3]. Besides, IM3 assessment does not perfectly describe the multicarrier modulation signal with harmonics and potentially cross-modulation

products originating from the numerous subcarriers of the modulating signal. A proper choice of modulation power for a DMT signal is more complicated than for an on-off keying (OOK) due to the internal characteristic amplitude of the signal, which follows a Gaussian distribution, as shown in Figure 2.

Figure 2: Histogram of the transmitted DMT Signal.

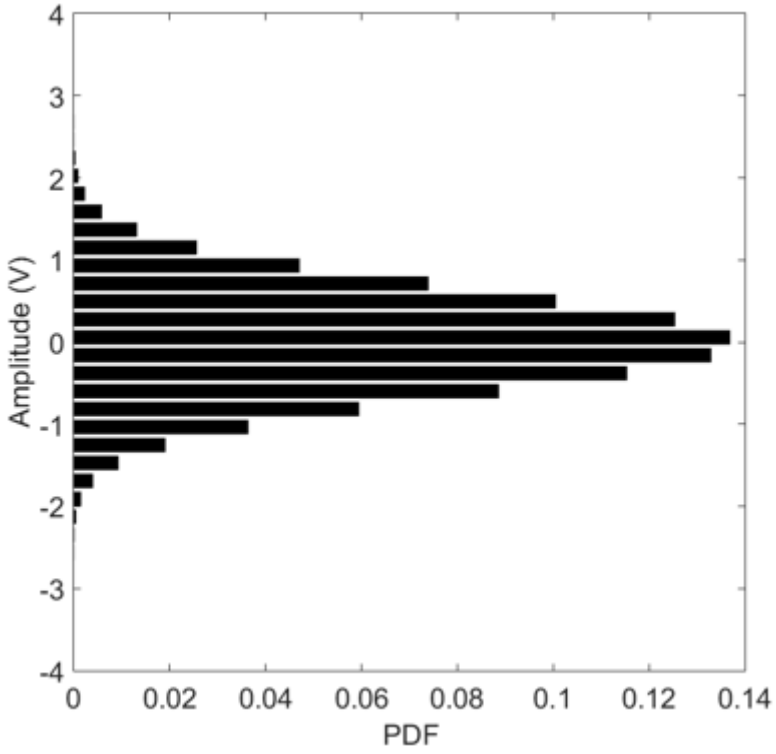

An assessment based on the SNR allows the optimization of the LED operating conditions. Since A/D conversions can clip the signal, it may contribute to signal degradation. Then, one can benefit from choosing the maximum amplitude of the DAC without clipping the signal. Otherwise, one should find an optimal compromise between distortions due to clipping effects and SNR improvements. Coming from higher levels of modulation power, it is also crucial to perform such optimization before proceeding to measurements with the optical emitter.

An increase on the radiofrequency (RF) power may be responsible for higher-order harmonics and intermodulation distortions in the optical signal. The RF power is also related to the SNR, then, the optimum points of bias and RF power, measurements were found by following a measured power-current curve, which is obtained by the use of the SNR_{mc} as a performance metric.

$$\max_b \sum b_n$$

$$\text{s.t.} \quad e_n(b_n) < E_t, \qquad (1)$$

where b_n is the number of bits used in the n^{th} sub-channel, e_n is the energy used in the transmission of b_n and E_t is the constraint on the total energy.

Original Levin Campello (LC) article [20] defines that a bit-loading algorithm is efficient if $\Delta e_n(b_n) \leqq \Delta e_m(b_m+1)$, for all n, m, where $\Delta e_n(b_n) = e_n(b_n)-e_n(b_n-1)$, for $b_n \geq 1$, and $\Delta e_n(b_n) = e_n(b_n)-e_n(0)$, for $b_n < 1$. In [20], an algorithm is E-tight if $0 < E_t - \Sigma_n\ e_n(b_n) < \min_m\ \Delta e_m(b_m+1)$. As shown in [20], the solution to the LC algorithm should be optimized such that LC is both efficient and E-tight.

LC is then a two-phase greedy algorithm that performs bit loading at each subcarrier according to the measured SNR in order to maximize the transmission rate. The algorithm starts with a probing step with the objective to improve the efficiency of the bit distribution. The bit distribution is considered to be efficient when there is no possible change of a bit from one subcarrier to another that would reduce the total energy of the DMT symbol. The information of SNR per subcarrier is used at an additional step which is necessary to adapt the total DMT symbol bit-rate with respect to the energy constraint. The second phase of the algorithm enhances the performance by make the system E-tight.

In multi-level optical transmission systems, the bias current and the amplitude of modulating signal are chosen to operate in the linear region of the transfer function of the optical source [4]. If the system operates outside this region, the modulated signal can be clipped and it may suffer distortions coming from the non-linear electro-optical conversions which lead to both degradations in the signal SNR and to out-of-band noise that could potentially degrade signals in neighbouring frequencies. As mentioned before, the time-domain DMT signal follows a Gaussian distribution. Moreover, the probability that signal amplitude, due to a high peak-to-average power ratio (PAPR), exceeds the maximum DAC output voltage is proportional to the number of subcarriers and the QAM level of the subcarriers [1]. Thus, setting the DMT signal amplitude is not as simple as multiplying a normalized signal by a constant. As a matter of fact, the signal is rescaled according to a target power P_t that is a function of the DAC maximum peak-to-peak voltage $V_{pp,max}$, as in the following.

$$P_t = \left(\frac{V_{pp,max}}{2SF}\right)^2, \qquad (2)$$

where SF is the scaling factor of the DMT signal. The rescaled DMT signal $s_r(t)$ can be written as:

$$s_r(t) = s(t)\sqrt{\frac{P_{DMT}}{P_t}}, \quad (3)$$

where P_{DMT} is the normalized power of the DMT signal.

Figure 3 shows a high degree of non-linearity on the Power-to-current relation in our FFOS. If the optical power in dBm scale is approximated by a linear regression of the current, the mean square error (MSE) is 2.07 dB. This non-linearity degrades the transmission performance, which may be mitigated by an approach based on the SNR_{mc} [4].

Figure 3: Optical output power as a function of the bias current of the 560 nm FFOS.

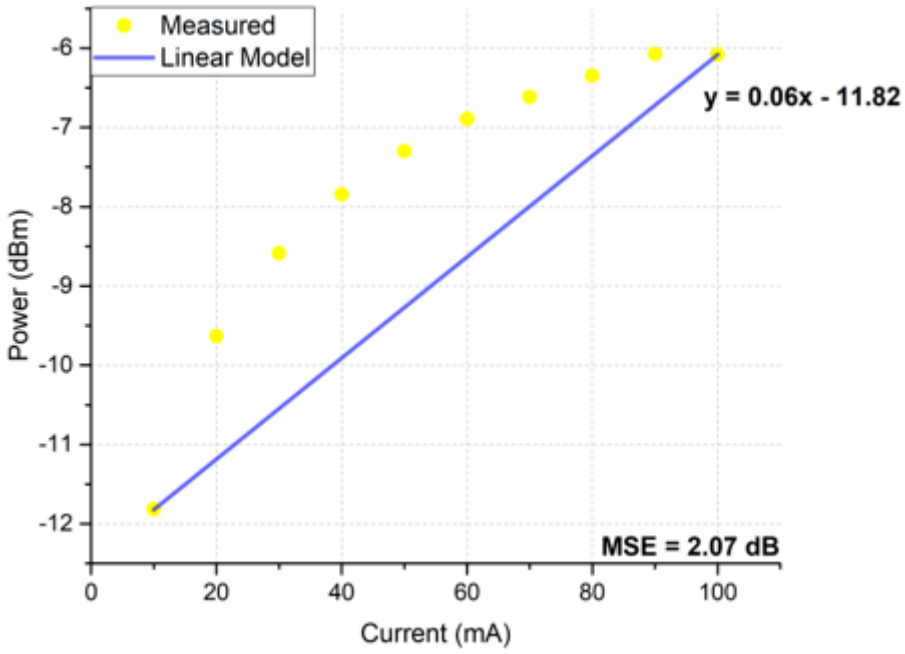

The spectral characteristic of the optical sources used in the experiment is shown in Figure 4, where its full width at half maximum (FWHM) is 31 nm.

Figure 4: Optical output power as a function of the wavelength for a 560-nm FFOS.

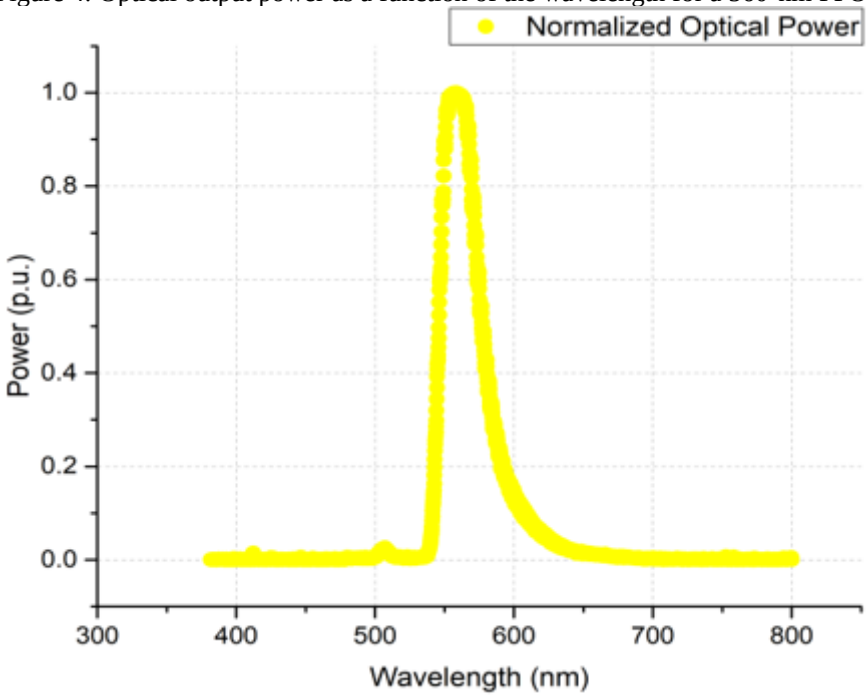

The DAC might also clip the signal thus contributing to signal degradation due to non-linear conversions. Following the same principle mentioned with regard to the LED, the idea is to benefit the most from the amplitude of the DAC without clipping the signal or to find a compromise of distortions coming from the clipping effects and SNR improvement related to high modulating power. It is important to perform such optimization before proceeding to the measurements with the optical emitter so that the distortion coming from different blocks in our transmission chain (DAC, electrical amplifiers and the optical emitter) can have its effects isolated without influence from the degradations coming from the electrical devices. Some non-linearities of the channel were previously analyzed in [4].

The use of a source bandwidth larger than the channel bandwidth may generate frequency-selective distortions. Although DMT mitigate frequency-selective effects, placing the source response on a highly attenuated range may lead to unrecoverable distortions. Figure 5 illustrates the frequency response of the system measured using a network analyzer. The measured 3-dB frequency f_{3dB} was 12 MHz as described in table 1. Despite the system bandwidth of 12 MHz, the authors choose the DMT signal bandwidth B = 20 MHz in order to improve the SNR.

Figure 5: Power spectrum of the transmission chain.

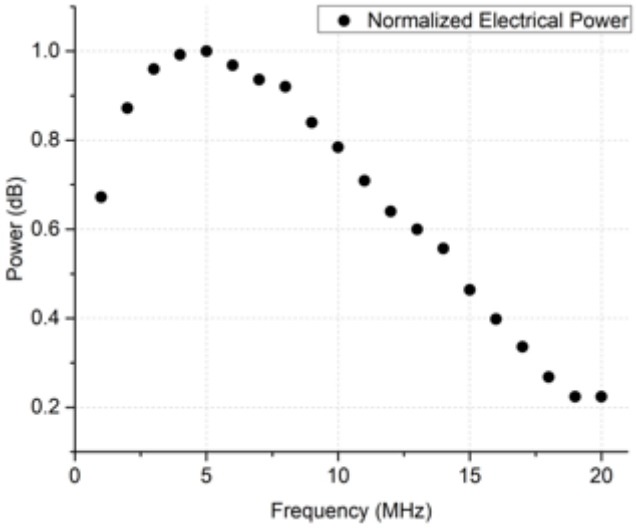

3 EXPERIMENTAL SETUP

The experimental setup [2], [3], [4] consists of a computer that performs DMT modulation/demodulation, an arbitrary function generator Tektronik AFG3251, which works as a DAC, a bias-T Mini-Circuits ZG85-12G+, a DC source ICEL Manaus 1500, the fluorescent optical source operating at 560 nm [1], 20 m of Eska Mitsubishi SI-POF, a fixed gain photodetector Thorlabs PDA10A and a digital storage oscilloscope (DSO) Rohde & Schwarz RTO 1002 to digitize the received signals.

Figure 6: The experimental setup used for acquiring data.

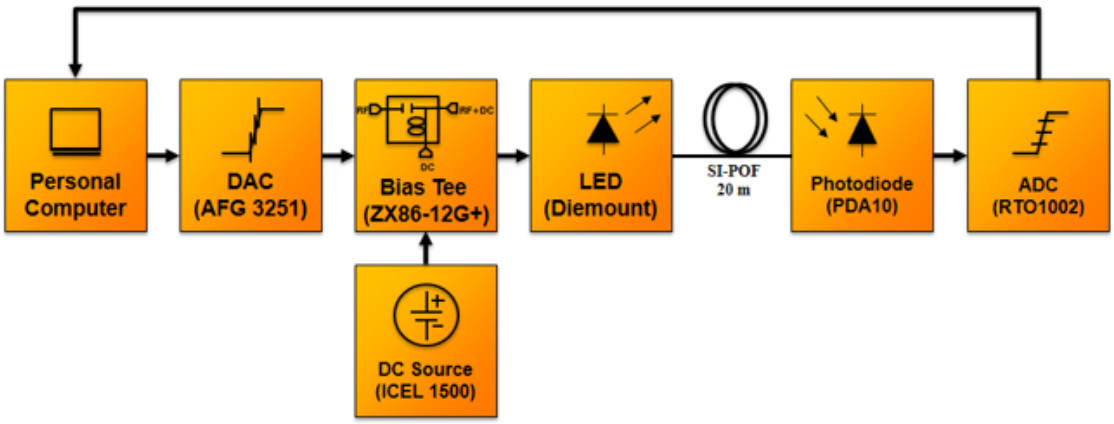

Other transmissions were made using a baseband signal that consists of a 20 MHz real-valued DMT signal with 491 useful subcarriers. The IFFT length is 984, when DC and Nyquist null subcarriers are considered. Moreover, 16 samples per DMT symbol are used as a CP. The total DMT symbol duration is 25 μs, where the useful data occupies 24.6 μs and 0.4 μs represents the guard interval. DAC and ADC operate at 100 MSa/s and

200 MSa/s respectively. Then, some metrics such as SNR, root-mean square error vector magnitude (EVMRMS) and BER per subcarrier are used to assess the system over 1,000 DMT symbols. The operation bias was set within the range 10 mA to 100 mA and the scaling factors of the DMT signal ranges from 22 dB to 32 dB, which implies voltages in the order of 1 to 10 Vpp. To find the optimal amplitude at the output of the DAC, the SF was varied in electrical back-to-back (EB2B) and the SNR_{mc} [19] was measured:

$$SNR_{mc} = \Gamma\left[\left(\prod_{i=1}^{N_D}\left(1+\left(\frac{SNR_i}{\Gamma}\right)\right)^{(1/\Gamma)}\right)-1\right] \quad (4)$$

where N_D is the number of data subcarriers, SNR_k is the SNR of each subcarrier and Γ is the gap to the capacity, which is the capacity of an equivalent mono-carrier transmission, and it was empirically set to 5 dB. SNR_{mc} denotes a single SNR metrics characterizing the set of sub-carriers by an equivalent Additive-White-Gaussian-Noise (AWGN) channel achieving the same data rate as the DMT system[19].

Table 1: Summary of DMT transmission system parameters.

Symbol	Description	Value
f_{DAC}	DAC Sampling Rate	100 MSa/s
f_{ADC}	ADC Sampling Rate	200 MSa/s
B	DMT Signal Bandwidth	20 MHz
N_{uscr}	Number of Useful Subcarriers	491
T_{DMT}	Total DMT Symbol Duration	25 µs
N_{cp}	Samples per cyclic prefix	16
L	Fiber Length	20 m
f_c	Bias Tee cut-off frequency	0.2 MHz
f_{3dB}	System 3 dB Frequency	12 MHz
L_{FPOF}	FPOF Length	14.5 mm
α_{560}	Attenuation coefficient at 560 nm	70 dB/km

4 RESULTS

The first step of the transmission is to send the probe signal to characterize the SI-POF channel. The resulting SNR_{mc}, spectrum and time-domain plots of the received DMT signal, for some values of SF and bias current, are respectively shown in Figures 7, 9 (a, b, and c) and 10 (a, b, and c). Figure 9 also shows an example of the received signal in the time domain with 80 DMT symbols. The assessment of the SNR_{mc} as a function of SF and the current bias are presented at figure 8, providing the overall performance of the FFOS with a DMT signal.

Figure 7 shows the curve levels of SNR_{mc} as a function of the current bias and SF, where one can observe the optimal performance with different bias currents using 20

m of POF and the FPOF in the linear range of the DAC evaluated at [4], from 10 mA to 100 mA and an SF range of 22 dB to 32 dB. The plot of those level curves is denominated as a whole as cartography. It can be seen that the optimal SNR_{mc} occurs when the current bias lies between 70 and 100 mA, and the SF is between 22 and 24 dB. This result is due to the fact that the optical power output of the FFOS increases proportionally to the DC current and the amplitude of the signal.

Figure 7: Cartography and elliptical fitting.

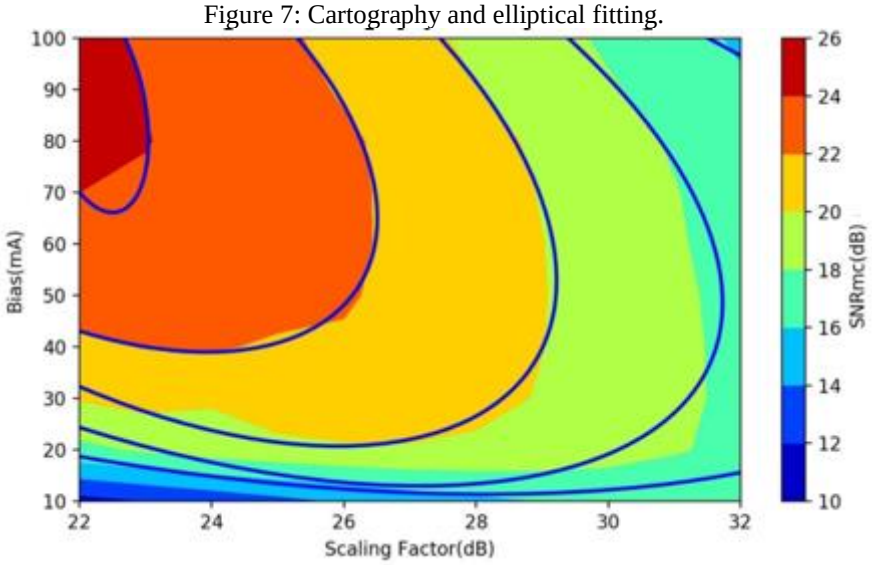

One can observe that the relation between RF and SNR is not monotonic. Since the increase of the power of the optical source may not result in an increase of the SNR due to clipping. The received signal at the DSO for an SF of 22 dB and 10 mA is clipped inferiorly and superiorly for a SF of 22 dB and 100 mA of current bias, respectively. It is also measured that a bias of 50 mA and 22 dB, where the signal is not clipped.

Table 1: Parameters of the fitted ellipses.

Center	Width	Height	Φ (°)	Focus 1	Focus 2
[22.2, 87.5]	0.8	21.5	0.8	[22.5, 66.1]	[21.9, 109.0]
[21.4, 90.6]	4.4	51.6	2.8	[23.9, 39.2]	[18.9, 141.9]
[22.4, 87.4]	5.8	66.8	3.1	[25.9, 21.0]	[18.8, 153.9]
[21.9, 89.4]	8.3	76.6	4.0	[27.2, 13.4]	[16.6, 165.3]
[21.8, 79.5]	12.1	68.4	5.5	[28.3, 12.4]	[15.4, 146.5]

Figure 8: Extrapolation of the elliptical fitting on the SNR_{mc} cartography.

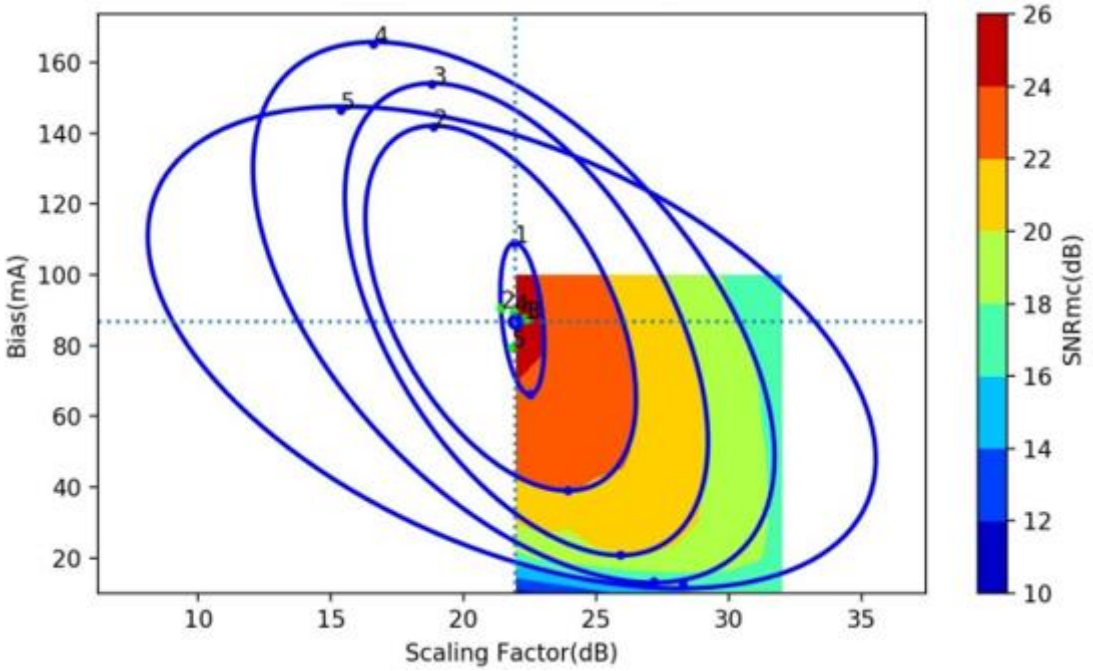

Figure 9: Time-domain received DMT signal assesment.

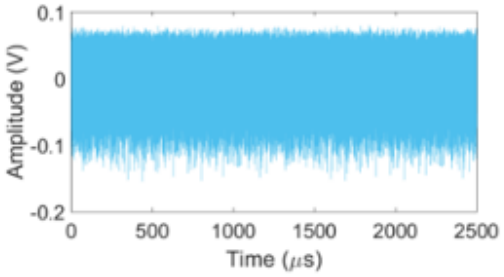

(a) Time-domain DMT signal for a bias current of 10mA, SF of 22dB and $SNR_{mc}$of 10dB.

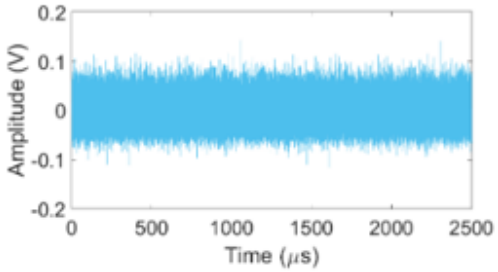

(b) Time-domain DMT signal for a bias current of 50mA, SF of 22dB and $SNR_{mc}$of 10dB.

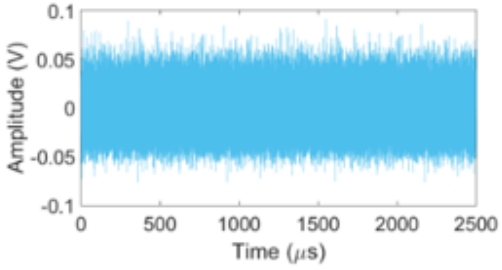

(c) Time-domain DMT signal for a bias current of 90mA, SF of 22dB, and $SNR_{mc}$of 10dB.

Figure 10: Assessment of the received DMT signal spectrum.

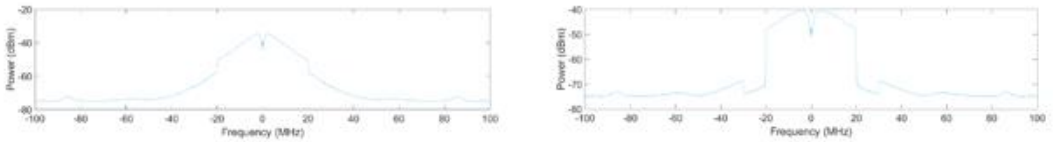

(a) Spectrum of DMT signal for a bias current of 10 mA, SF of 22dB and $SNR_{mc}$of 10 dB.

(b) Spectrum of DMT signal for a bias current of 50 mA, SF of 22 dB and $SNR_{mc}$of 10 dB.

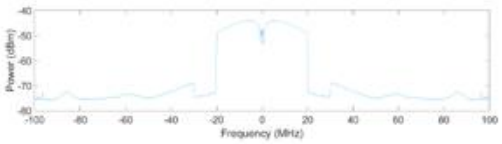

(c) Spectrum of DMT signal for a bias current of 90mA, SF 22dB,SNR_{mc}10dB

We approximated the measured cartography by ellipses using the least mean squares as metric. The ellipsis parameters are described in table 2. The point with the highest SNR was calculated as the centroid of the ellipsis at the coordinates [21.94, 87.53]. In figure 8, one can observe the extrapolation of the measurements using the \snrmc as metric. Our perspective is to provide a numerical model to predict the optimal operation point of the optical source avoiding a sub-optimal operation. The best value for the mean-absolute error (MAE) is 6.7.

The use of ellipsis level curves lead us to a three-dimensional (3-D) ellipsoid model, as represented in Fig.11. The MAE for the whole ellisoid is 26.7.

Figure 11: 3-D Ellipsoid fitting.

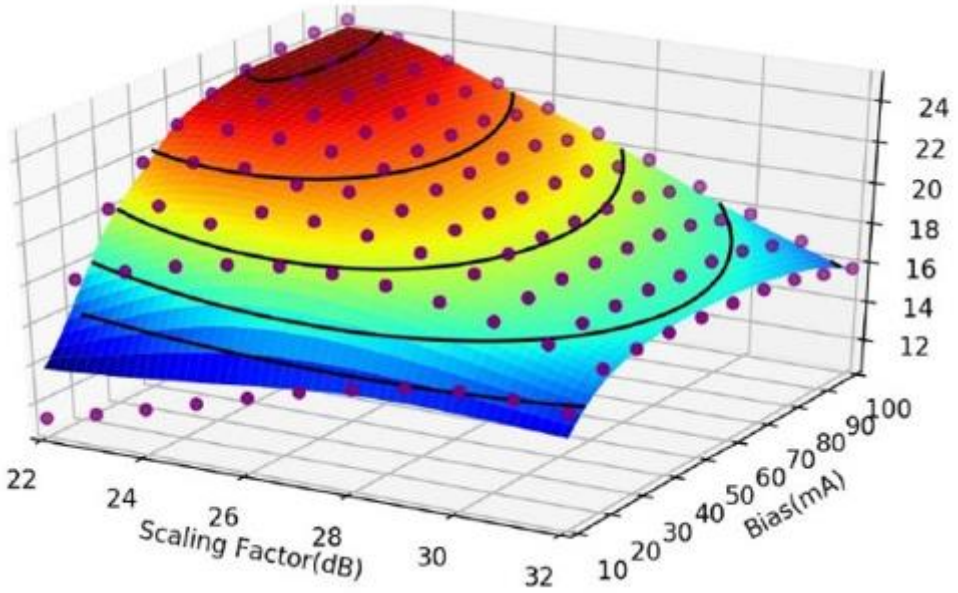

5 CONCLUSION

This work analyzes the effects of non-linear distortion on a DMT system with a FFOS operating at 560 nm for 20 m for SI-POF. We propose a numerical model of our channel based on an experimentally evaluation using a methodology based on the evaluation of multicarrier SNR (SNR_{mc}) of a DMT signal that could be extrapolated to any device submitted to nonlinear distortions, including a DAC. This method is then extrapolated to take into account the biasing current of the light source as well. An SNR_{mc} cartography can thus be used to find the optimal biasing and modulating conditions of the light source. An analysis of the non-linear effects in our optical emitter was performed, which resulted in the approximation by ellipsis of our channel cartography based on \snrmc for a DMT system with 560 nm FFOS source.

REFERENCES

[1] R M Ribeiro, VNH Silva, APL Barbero, CM Alves and CRL Rodrigues, Electronics Letters, vol. 51, pp. 168–170, 2015, ISSN 0013-5194.

[2] FAN Sampaio, VNH Silva, LA Neto, APL Barbero, RM Ribeiro and TN Ferreira, "A fast fluorescentlight source for data communication over si-pmma-pof" in Proc. of Internat. Conf. Plastic Optical Fibres, pp. 1-3, Birmingham, UK, 2016.

[3] FAN Sampaio, VNH Silva, LA Neto, TN Ferreira, APL Barbero and RM Ribeiro, "Highly spectrally efficient discrete multi-tone transmission over step index PMMA optical fibre for short-range optical communication," Journal of Communication and Information Systems, vol. 33, pp. 250–256.

[4] FAN Sampaio, VNH Silva, TN Ferreira, APL Barbero, RM Ribeiro, LA Neto and TVN Coelho, "Analysis of 560-nm led linearity on dmt transmission over step-index pmma optical fibre", in Proc. IEEE British and Irish Conference on Optics and Photonics (BICOP), pp. 1-4, London, UK, 2016.

[5] S. C. J. Lee, F. Breyer, S. Randel, R. Gaudino, G. Bosco, A. Bluschke, M. Matthews, P. Rietzsch, R. Steglich, H. P. A. van den Boom, and A. M. J. Koonen , "Discrete Multitone Modulation for Maximizing Transmission Rate in Step-Index Plastic Optical Fibers," Journal of Lightwave Technology, vol. 27, n. 11, pp. 1503-1513, 2009.

[6] R. Kruglov, J. Vinogradov, O. Ziemann, S. Loquai and C. Bunge, "10.7-Gb/s Discrete Multitone Transmission Over50-m SI-POF Based on WDM Technology", IEEE Photonics Technology Letters, vol. 24, n. 18, pp. 1632–1634, Sept. 2015.

[7] R. Kruglov, S. Loquai, J. Vinogradov, O. Ziemann, C. Bunge, G. Bruederl and U. Strauss, "10.7 Gb/s WDM Transmission over 100-m SI-POF with Discrete Multitone," in Proc.of Optical Fiber Communication Conference, pp. 1-3, Anaheim, Mar. 2016.

[8] V. D. Trong, P. H. Binh and T. C. Thang, "A 622 Mbit/s transmitter for POF-based home networks using red LED," in Proc. IEEE Fifth International Conference on Communications and Electronics (ICCE), pp. 30-33, 2014, Da Nang, July 2014.

[9] R. Nazaretian and GM Molen, "Reducing vehicle weight and improving security by usingplastic optical fiber," in Proc. IEEE Vehicle Power and Propulsion Conference (VPPC), Montreal, pp. 1-4, 2015.

[10] Y. Shi, E. Tangdiongga, AMJ Koonen, A. Bluschke, P. Rietzsch, J. Montalvo, MM de Laat, GN van den Hoven and B. Huiszoon, "Plastic-optical-fiber-based in-home optical networks," IEEE Communications Magazine, vol. 52, n. 6, pp. 186-193, 2014.

[11] O. Ziemann and L. Bartkiv, "Pof-wdm, the truth," Proc. 20th International Conference on Plastic Optical Fibers, pp. 1-2, Edinburgh, UK, Oct 2009.

[12] PJ Pinzón, IP Garcilópez and C. Vázquez, "Efficient Multiplexer/Demultiplexer for Visible WDM Transmission over SI-POF Technology," Journal of Lightwave Technology, vol. 33, n. 7, pp. 3711-3718, 2015.

[13] P. Bienias, G. Budzyn and E. Beres-Pawlik, "Wdm for application in passive pof lan networks," in Proc. International Conference on Transparent Optical Networks (ICTON), pp. 1-4, Trento, July 2016.

[14] S.C.J. Lee, F. Breyer, S. Randel, R. Gaudino, G. Bosco, A. Bluschke, M. Matthews, P. Rietzsch, R. Steglich, H.P.A. van den Boom and A.M.J. Koonen, "Discrete Multitone Modulation for Maximizing Transmission Rate in Step-Index Plastic Optical Fibers," Journal of Lightwave Technology, vol. 27, n. 11, pp. 1503-1513, 2009.

[15] M. Joncic, R. Kruglov, M. Haupt, R. Caspary, J. Vinogradov and U.H.P. Fischer, "Four-Channel WDM Transmission Over 50-m SI-POF at 14.77 Gb/s Using DMT Modulation," IEEE Photonics Technology Letters, vol. 26, n. 13, pp. 1328-1331.

[16] B. Charbonnier, P. Urvoas, M. Ouzzif and J. Le Masson, "Capacity optimisation for optical links using DMT modulation, an application to POF," Proc. European Conference on Optical Communication, pp. 1-2, Brussels, Sept 2008.

[17] X. Li, N. Bamiedakis, J. J. D. McKendry, E. Xie, R. Ferreira, E. Gu, M. D. Dawson, R. V. Penty and I. H. White, "11 Gb/s WDM Transmission Over SI-POF Using Violet, Blue and Green μLEDs," Proc. Optical Fiber Communication Conference, pp. 1-4, Anaheim, Mar 2016.

[18] R. Caspary, M. Joncic, M. Haupt, U. Fischer-Hirchert, R. Kruglov, J. Vinogradov, H. Johannes and W. Kowalsky, "High speed WDM transmission on standard polymer optical fibers," in Proc. 17th International Conference on Transparent Optical Networks, pp. 1-4, Budapest, July 2015.

[19] L. Anet Neto, Etude des Pontentialites des Techniques de Modulation Multiporteuse pour les Futurs Reseaux D'Acces Optique WDM et TDM PON, Ph.D. Thesis, Université de Limoges, 2012.

[20] J. Campello, "Optimal Discrete Bit Loading for Multicarrier Modulation Systems," in Proc. IEEE International Symposium on Information Theory, pp. 193-194, Cambridge, USA, Aug. 1998.